Analysis of laminar properties of electron beam in traveling wave tube based on *K*-means clustering algorithm*

SHEN Changsheng, ZHANG Tianyang, BAI Ningfeng, CHEN Zhaofu, FAN Hehong, SUN Xiaohan

Research Center for Electronic Device and System Reliability, School of Electronic Science & Engineering, Southeast University, Nanjing 210096, China

Abstract

In order to improve the stability and reliability of the traveling wave tube (TWT), the optimization and design of the electron beam have become a key part in vacuum electronic devices. Laminar properties are a key parameter for evaluating the quality of the electron beam. The transverse displacement of the particles in the laminar electron beam is proportional to the transverse velocity. In the phase space distribution image of non-laminar properties electrons at a certain position, there is no linear relationship between the transverse displacement and the transverse velocity. The energies of particles in the electron beam are different, so the particles have different initial velocities. The particle source at the electron beam waist in the electron gun is used as a particle source for the beam wave interaction simulation. The output characteristics of the TWT more closely resemble the actual ones. A method of simplifying the particles at the electron gun beam waist into macroparticles using the *K*-means clustering algorithm is proposed. The macroparticle is used as a particle source in the TWT interaction zone for simulating the beam wave interaction, which reduces the simulation time from 5.53 to 0.65 h and improves the simulation efficiency. Compared with the original particle, both the simplified particle generated by the *K*-means clustering algorithm and the simplified particle generated by the mesh model greatly reduce the computational load of the interaction zone simulation. Compared with the results from the grid model, the simulation results of the beam-wave interaction of macroparticles, obtained by using the *K*-means clustering algorithm, are closer to those of the beam-wave interaction, obtained by using the original particles. By adjusting the cathode divergence angle and the distance between the anode and cathode of the electron gun of a certain type of TWT, the

* The paper is an English translated version of the original Chinese paper published in Acta Physica Sinica. Please cite the paper as: SHEN Changsheng, ZHANG Tianyang, BAI Ningfeng, CHEN Zhaofu, FAN Hehong, SUN Xiaohan, **Analysis of laminar properties of electron beam in traveling wave tube based on *K*-means clustering algorithm.** *Acta Phys. Sin.*, 2025, 74(18): 188401. DOI: 10.7498/aps.74.20250765

simulation results show that when the divergence angle is adjusted within a range of 0°–1°, the larger the divergence angle, the larger the radial root mean square emittance value, the worse the laminar properties of the electron beam, and the power of the output signal of the TWT decreases. When the distance between the anode and cathode is adjusted within a range of 0.8–1.6 mm, the radial root mean square emittance decreases from 2.51 to 2.22 mm·mrad, the laminar properties of the electron beam are improved. The output power of the TWT increases from 328.34 to 414.10 W, and the operating frequency bandwidth with an output power greater than 300 W is expanded from 3 to 5 GHz. Therefore, the particle simplification model using the *K*-means clustering algorithm improves the simulation efficiency of the beam wave interaction. Based on the influence of the laminar properties of the electron beam on the performance of the TWT, the structural parameters of the electron gun can be optimized.

Keywords: traveling wave tube,electron beam laminar property,K-means clustering algorithm,radial rms-emittance

PACS：84.40.Fe

doi: 10.7498/aps.74.20250765

cstr: 32037.14.aps.74.20250765

1. Introduction

Traveling wave tube (TWT), as the core device of microwave signal amplification, is widely used in electronic countermeasures, radar detection, wireless communication, aerospace and other fields because of its high working frequency, high output power, wide working frequency band and strong anti-interference ability[1]. As of December 2023, Xi'an Institute of Space Radio Technology, as an integrator of the whole machine, has applied 566 domestic traveling wave tube amplifiers in orbit, with operating frequencies ranging from L band to Q/V band and continuous wave output power ranging from 10 W to 200 W[2]. The main components of a traveling wave tube include an electron gun, a slow wave structure and a collector. The electron beam generated by the electron gun is used as the particle source in the traveling wave tube. The slow wave structure is used to reduce the phase velocity of the microwave signal, so that the electron beam can interact effectively with the microwave signal. The main function of the collector is to receive the particles that have completed the energy exchange with the microwave signal. Clustering algorithm is a basic tool in machine learning, data mining and pattern recognition, which is used to divide a data set into several subsets so that the samples in the same subset are similar and the samples in different subsets are dissimilar[3]. In recent years, more and more complex clustering algorithms have been applied to various industrial scenarios, such as density peak clustering[4] enhanced by density normalization, grid-based density peak clustering algorithm[5], wavelet-based load curve

clustering algorithm[6], etc. Among these, *K*-means clustering algorithm is one of the most popular and simplest clustering algorithms. First introduced in 1955, it continues to be widely used despite the publication of thousands of clustering algorithms since[7]. In the beam-wave interaction simulation of TWTs, a uniform ideal electron beam is usually used as the particle source, and the actual electron gun is replaced by setting appropriate voltage, current, electron beam radius, etc., which has the advantage of shortening the beam-wave interaction calculation time. However, when an ideal electron beam is used as the particle source, the influence of electron beam inhomogeneity on beam-wave interaction is often neglected because the energy and distribution of each particle on the ideal electron beam are uniform[8]. In practice, the design of the electron gun is insufficient, which not only makes the current and the radius of the electron beam not reach a good pre-value, but also makes the initial velocity of each particle different because of the difference of the energy of each particle in the electron beam. Some particles are synchronized with the microwave signal, while others do not, affecting the overall beam-wave interaction. Using particles from the beam waist of the electron gun as the particle source of the beam-wave interaction simulation, the output characteristics of TWT are closer to real conditions. However, the electron beam contains hundreds of particles, making the simulation computationally expensive. Therefore, a clustering algorithm is introduced into the simulation analysis of the TWT electron beam. The simple *K*-means clustering algorithm is used to divide thousands of particles at the waist of the electron gun into a smaller number of macroparticles, ensuring that the distribution of macroparticles resembles that of the original particle group. These simplified macroparticles can be used as the particle source in the TWT interaction region for beam-wave interaction simulation.

The laminar nature of the electron beam of TWT affects the stability of the electron beam transmission in the periodic focusing structure and the gain of the output signal[9]. Laminarity is primarily characterized by the degree of orbital crossing. A non-uniform distribution of particle orbit inclinations and excessive transverse velocity components can cause electron trajectory crossing and lead to some particles impinging on the TWT helix during transmission. This reduces the number of particles available for energy exchange with the high-frequency field, ultimately affecting key TWT performance indicators such as gain, bandwidth, and output power.

In recent years, advances in simulation technology and computing power have led to significant progress in electron beam research. In the field of electron optics and beam-wave interaction, establishing a bridge between realistic electron beam conditions and beam-wave interaction simulations is essential to ensure high consistency between TWT design and experimental results. Ge et al.[10] use MATLAB to process the macroparticle data at the beam

waist, which was then used as the particle source for simulating the TWT interaction region, meeting the requirements of the interactive calculation model. Due to the complex electromagnetic environment and the randomness of the cathode emission in helix TWTs, the velocity and direction of the electron beam from the electron gun to the slow wave structure are non-uniform. In our previous work, two parameters, the velocity amplitude fluctuation range and the velocity direction fluctuation range, were used to characterize the output characteristics of the helix TWTs under different electron beam velocities[11]. A simulation model was established to analyze the influence of non-uniform electron beam velocity on TWT performance. In the study of evaluating the electron beam quality, Louksha et al.[12] investigated the effect of cathode surface roughness on the electron beam quality in a gyrotron electron optical system by continuously simulating variations in the transverse velocity v_x at a small distance from the cathode surface. In view of the lack of quantitative evaluation parameters for electron beam laminarity in existing electron optics software, Zhang et al. proposed a new method using crossover rate and fluctuation rate[13]. Simulation results showed that the crossover rate index can accurately and quantitatively evaluate the laminar quality of the electron beam . When the crossover rate is less than 3% and the fluctuation rate is less than 30%, the designed electron optical system meets the engineering requirements. David et al.[14] studied the design of electron gun using computer optimization technology, and used MATLAB to program and calculate the simulation results. To evaluate electron beam laminarity, they used the first and second derivatives of particle trajectories to form an objective function for optimizing the laminar characteristics of the simulated electron beam. Liu et al.[15] proposed a rotating surface cathode design to improve the laminar flow of the concentrated electron beam. Through simulation experiments, the radial distribution of the electron beam current density in the electron gun was observed, which showed that the rotating surface cathode could reduce the spherical aberration and help to improve the quality of the electron beam.

Few studies in the literature have simulated the electron gun and TWT as an integrated system. In this paper, the performance of a TWT[16] with a three-clamped helix slow-wave structure (SWS) is simulated and analyzed. When particles at the beam waist of the electron gun are used as the TWT particle source, the initial particles are simplified into fewer macroparticles using the *K*-mean clustering algorithm. These macroparticles are then used as the particle source of the beam-wave interaction simulation of the traveling wave tube. Radial root-mean-square (RMS) emittance is used to characterize the laminarity of the cylindrical electron beam, replacing subjective judgments based on magnified visual inspection of particle orbits. By optimizing the structural parameters of the electron gun, the laminar flow of the electron beam is improved, thereby enhancing the output performance of the TWT.

2. Theoretical model

2.1 Phase space model

The phase space model provides an intuitive comparison between laminar and non-laminar electron beams. During the generation and transmission of electron beam from the electron gun, the position and velocity of each particle change continuously.. In a rectangular coordinate system, the motion state of each particle can be represented in a six-dimensional phase space of x, v_x, y, v_y, z, v_z. When the particle distribution of the electron beam cross section is circularly symmetric, the particle state can be represented by a two-dimensional phase space of x, v_x. By plotting x as the abscissa and v_x as the ordinate, a phase space distribution including the transverse displacements and velocities of all particles can be obtained [17]. The laminarity of the electron beam essentially reflects the degree of order or disorder of particle orbits during beam transmission.

The Fig. 1 is an ideal two-dimensional electron beam model, illustrating three particle orbits and the corresponding phase space distribution during the transport of a laminar electron beam. The model temporarily ignores the space charge effect and external forces. The beam extends infinitely in the z-direction. The origin of coordinates is chosen such that the x axis begins at the center of the electron beam, and the rate of change of the transverse displacement is the transverse velocity v_x.

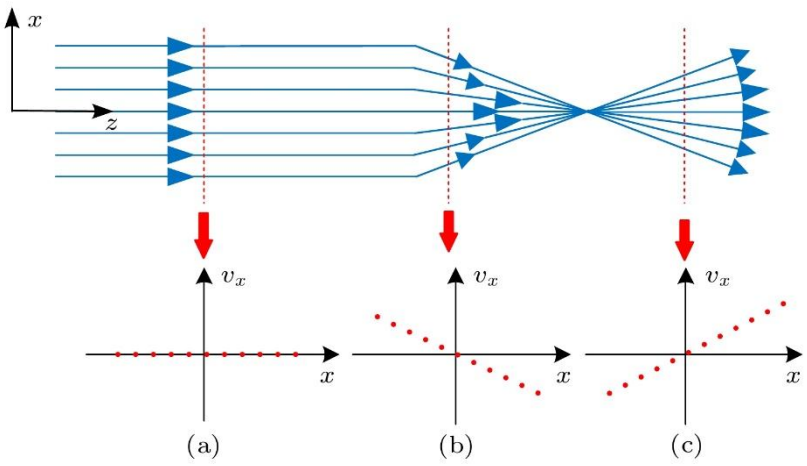

Figure 1. Orbital conditions of three types of laminar electron particles and the corresponding phase space distribution diagrams: (a) Parallel electron beam; (b) convergent electron beam; (c) divergent electron beam.

Where Fig. 1(a) is the parallel electron beam, that is, the transverse velocity of all particles is 0, and the particle orbits remain layered throughout beam generation and transmission, with no crossing trajectories. The Fig. 1(b) is a convergent electron beam, and all the particle orbits converge to one point, because the transverse displacement of the particle is proportional to the transverse velocity. The Fig. 1(c) is a divergent electron beam, and the transverse displacement of the particle is proportional to the transverse velocity. Even if the particle is transported to an infinite distance, the orbits of the particle will not cross each other.

In the actual electron beam, there are particles with transverse velocity at any transverse position, which are disordered in the process of generation and propagation, so that the trajectories of particles will continue to cross each other, so the actual electron beam is non-laminar. For a non-laminar electron beam shown by Fig. 2, there is no linear relationship between the transverse displacement and the transverse velocity in the phase space distribution image at a given position.

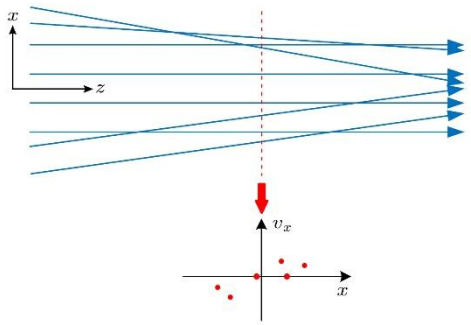

Figure 2. Orbital conditions of non-laminar electron beam particles and the corresponding phase space distribution diagrams.

2.2 Radial RMS emittance

In the electron gun design process, after calculating the electron trajectories for a given structure using numerical simulation software, designers typically assess the laminar flow of the electron beam by visual inspection [18]. This judgment is highly subjective, and even if the particle orbits at the waist are magnified, it is still challenging to identify their orbit crossing due to the large number of particle orbits. Therefore, quantitative parameters are needed to characterize the laminar state of the electron beam.

In experiments, the inclination angle of the particle orbit is usually easier to measure directly. The transverse displacement x and the transverse inclination x' are often used to calculate emittance. Emittance is a parameter that characterizes the area of the elliptical phase space region containing the particle distribution in trace space (x-x' plane). It is denoted by the symbol ε and expressed in units of mm·mrad, with its value defined as the area of the ellipse divided by π. The determination of the elliptical range is subject to errors, so the emittance

expression calculated based on the coordinate information of the particle trajectory in the electron beam is more practical. The emittance is described by the statistically defined emittance, that is, the root mean square of the transverse displacement of all particles, which is called the RMS emittance ε_{rms}.

Because the electron beam in a TWT is cylindrical, the radial RMS emittance $\varepsilon_{\text{r-rms}}$ can be used to characterize the laminar flow of the electron beam. To couple the laminar flow states in the *x* and *y* directions, a transformation from rectangular to polar coordinates is required. First, the RMS emittances in the *x* and *y* directions in the rectangular coordinates are derived .

The RMS emittance expression in the *x*-direction is[19]

$$\varepsilon_{x\text{-rms}} = \sqrt{\langle x^2 \rangle \langle (x')^2 \rangle - \langle xx' \rangle^2}. \tag{1}$$

Similarly, the RMS emittance in the *y*-direction of is

$$\varepsilon_{y\text{-rms}} = \sqrt{\langle y^2 \rangle \langle (y')^2 \rangle - \langle yy' \rangle^2}. \tag{2}$$

By coupling the *x* with the *y* direction, the radial RMS emittance can be used to characterize the laminar nature of the cylindrical electron beam. Tis requires transforming the rectangular coordinate system to the polar coordinate system.

Under the paraxial approximation, the relationship between the transverse inclination angle and the transverse velocity is $x' \approx v_x/v_y v_z v_z$ and $y' \approx v_y/v_y v_z v_z$, and the relationship between the RMS emittance and the transverse velocity can be obtained as

$$\begin{aligned} \varepsilon_{x\text{-rms}} &= \sqrt{\langle x^2 \rangle \langle (x')^2 \rangle - \langle xx' \rangle^2} \\ &= \sqrt{\langle x^2 \rangle \left\langle \left(\frac{v_x}{v_z} \right)^2 \right\rangle - \left\langle x \frac{v_x}{v_z} \right\rangle^2}, \end{aligned} \tag{3}$$

$$\begin{aligned} \varepsilon_{y\text{-rms}} &= \sqrt{\langle y^2 \rangle \langle (y')^2 \rangle - \langle yy' \rangle^2} \\ &= \sqrt{\langle y^2 \rangle \left\langle \left(\frac{v_y}{v_z} \right)^2 \right\rangle - \left\langle y \frac{v_y}{v_z} \right\rangle^2}. \end{aligned} \tag{4}$$

Fig. 3 is the vector map of particle velocity, where v_r is the radial velocity, while v_θ is the angular velocity. Using Fig. 3 to decompose the velocity in the direction of *x*, *y*, the radial velocity and angular velocity are obtained as

$$v_r = v_x \cos\theta + v_y \sin\theta, \tag{5}$$

$$v_\theta = v_x \sin\theta - v_y \cos\theta. \tag{6}$$

The relationship between the directional velocity of *x* and the radial and angular velocities can be obtained by solving the equations (5) and (6) simultaneously:

$$v_x = v_r \cos\theta + v_\theta \sin\theta, \tag{7}$$

$$v_y = v_r \sin\theta - v_\theta \cos\theta. \tag{8}$$

Substituting (7) into (3), we get:

$$\begin{aligned}\varepsilon_{x\text{-rms}} &= \left[\langle r^2\cos^2\theta\rangle \left\langle \left(\frac{v_r}{v_z}\cos\theta + \frac{v_\theta}{v_z}\sin\theta\right)^2\right\rangle - \left\langle r\cos\theta\left(\frac{v_r}{v_z}\cos\theta + \frac{v_\theta}{v_z}\sin\theta\right)\right\rangle^2\right]^{1/2} \\ &= \left(\frac{1}{N}\sum_{i=1}^{N} {r_i}^2 \frac{\cos 2\theta_i + 1}{2} \frac{1}{N}\sum_{i=1}^{N}\left[\left(\frac{v_r}{v_z}\right)_i^2 \frac{\cos 2\theta_i + 1}{2} + \left(\frac{v_\theta}{v_z}\right)_i^2 \frac{1-\cos 2\theta_i}{2} + \left(\frac{v_r}{v_z}\right)_i \left(\frac{v_\theta}{v_z}\right)_i \sin 2\theta_i\right]\right. \\ &\quad \left. - \left\{\frac{1}{N}\sum_{i=1}^{N}\left[r_i\left(\frac{v_r}{v_z}\right)_i \frac{\cos 2\theta_i + 1}{2} + r_i\left(\frac{v_\theta}{v_z}\right)_i \frac{\sin 2\theta_i}{2}\right]\right\}^2\right)^{\frac{1}{2}}.\end{aligned} \tag{9}$$

Substituting (8) into (4), we get:

$$\begin{aligned}\varepsilon_{y\text{-rms}} &= \left[\langle r^2\sin^2\theta\rangle \left\langle \left(\frac{v_r}{v_z}\sin\theta - \frac{v_\theta}{v_z}\cos\theta\right)^2\right\rangle - \left\langle r\sin\theta\left(\frac{v_r}{v_z}\sin\theta - \frac{v_\theta}{v_z}\cos\theta\right)\right\rangle^2\right]^{1/2} \\ &= \left(\frac{1}{N}\sum_{i=1}^{N} {r_i}^2 \frac{1-\cos 2\theta_i}{2} \frac{1}{N}\sum_{i=1}^{N}\left[\left(\frac{v_r}{v_z}\right)_i^2 \frac{1-\cos 2\theta_i}{2} + \left(\frac{v_\theta}{v_z}\right)_i^2 \frac{\cos 2\theta_i + 1}{2} - \left(\frac{v_r}{v_z}\right)_i \left(\frac{v_\theta}{v_z}\right)_i \sin 2\theta_i\right]\right. \\ &\quad \left. - \left\{\frac{1}{N}\sum_{i=1}^{N}\left[r_i\left(\frac{v_r}{v_z}\right)_i \frac{1-\cos 2\theta_i}{2} - r_i\left(\frac{v_\theta}{v_z}\right)_i \frac{\sin 2\theta_i}{2}\right]\right\}^2\right)^{1/2}.\end{aligned} \tag{10}$$

By further deducing (9) and (10), (11) can be obtained, which is the radial RMS emittance expression[20]:

$$\varepsilon_{r\text{-rms}} = \sqrt{\frac{(\varepsilon_{x\text{-rms}})^2 + (\varepsilon_{y\text{-rms}})^2}{2}} = \frac{1}{2}\left[\langle r^2\rangle\left(\left\langle (v_r/v_z)^2\right\rangle + \left\langle (v_\theta/v_z)^2\right\rangle\right) - \langle r\cdot v_r/v_z\rangle^2 - \langle r\cdot v_\theta/v_z\rangle^2\right]^{1/2}. \tag{11}$$

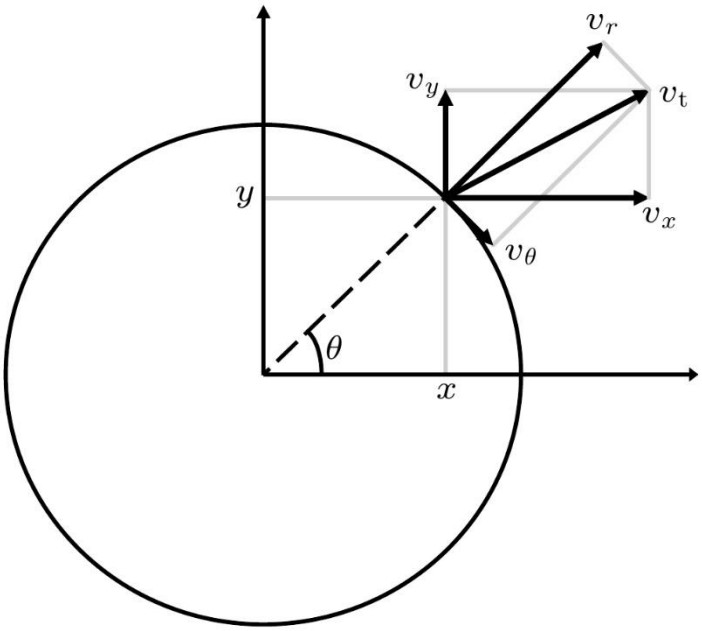

Figure 3. Vector diagram of particle momentum.

This section describes the state of particles in the electron beam and the phase space model. The phase space model is used as an example to distinguish the laminar electron beam from the non-laminar electron beam. Since the electron beam in the electron gun and the traveling wave tube is a cylindrical electron beam, the derived radial root-mean-square emittance can be used to characterize the laminar state of the electron beam.

2.3 *K*-means clustering algorithm

If thousands of original particles obtained from the electron gun simulation are all introduced into the particle source of the TWT for beam-wave interaction calculation and simulation by the particle introduction surface method, the computation time will be very long due to the huge calculation data, and the efficiency of the whole design optimization will be reduced. Therefore, the *K*-mean clustering algorithm is used to process the particle information at the beam waist in the electron gun, which is simplified into a smaller number of macroparticles to shorten the simulation time and improve work efficiency. The flow chart of that *K*-mean clustering algorithm applied to the electron beam simplification of the TWT is shown as a Fig. 4. This model is used to simplify the cross-sectional particles of the TWT electron beam into macroparticles, and includes the following steps: 1) Obtain the electron beam trajectory of the electron gun using a particle tracking solver, and extract information such as position distribution, velocity, and current of the cross-sectional particles at the beam waist. 2) Randomly select *K* particles from the cross-sectional particles at the beam waist as

macroparticles. 3) Calculate the distance between each cross-sectional particle and each macroparticle, and assign each particle to the region of the nearest macroparticle. 4) For all particles contained in the macroparticle region, respectively calculate the macroparticle positions in the *x* , *y*, and *z* directions, the velocities in the *x*, *y*, and *z* directions, the current values, as well as the mass and charge of the macroparticles. 5) Compare whether the position information of the newly calculated macroparticle in step 4 is consistent with that of the previous macroparticle. 6) If the position information is inconsistent, return to step 3 and continue solving for the new macroparticle positions until consistency is achieved; then terminate the loop and obtain the final macroparticle position distribution. 7) Use the processed macroparticles—including their velocities, current values, mass, and charge—as the particle source for the TWT interaction region, perform beam-wave interaction simulation, and obtain the output power of the TWT through analysis and calculation of the simulation results.

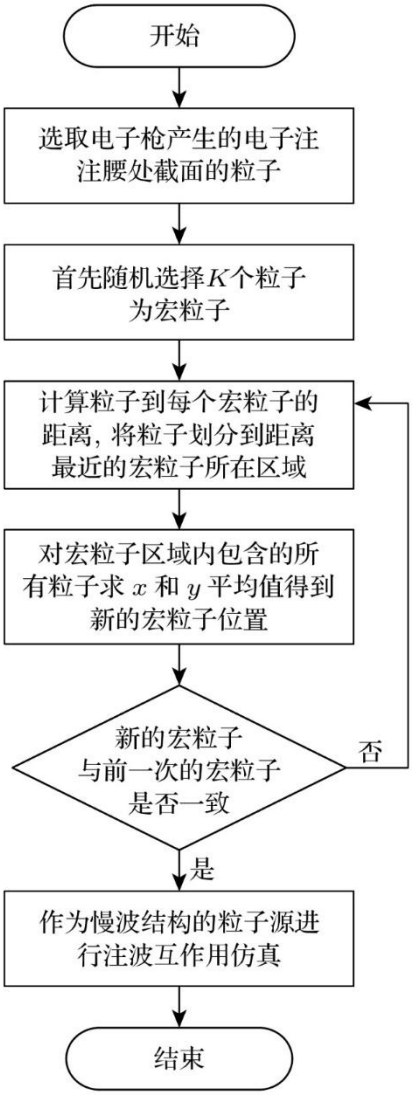

Figure 4. Simulation properties chart using the *K*-means clustering algorithm.

3. Simulation analysis

3.1 Traveling wave tube simulation flow

In this paper, a computer with 256G memory is used for TWT simulation analysis, and a GeForce RTX 4090D graphics card is employed in the CST simulations to enable GPU acceleration. The steps of TWT simulation analysis are shown in Fig. 5. After adjusting the parameters of the electron gun, the CST particle tracking solver is used to calculate the electron beam information with different laminar properties, and the radial RMS emittance is used to characterize the laminarity of the electron beam; In MATLAB, the *K*-mean clustering algorithm is used to simplify the particle information at the beam waist. The resulting macroparticles are used as the particle source in the TWT interaction region, and then the CST particle-in-cell solver is used to simulate the beam-wave interaction. Different levels of electron beam laminarity ultimately affect the output characteristics of the TWT. The parameters of the helix TWT used in this paper are listed in the Tab. 1.

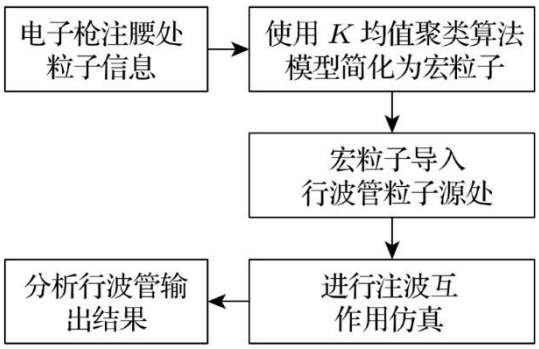

Figure 5. Steps of analyzing the TWT using the *K*-means clustering algorithm.

Table 1. Parameters of helical TWT.

Parameter Name	Parameter value
Working voltage/V	9600
Operating current/A	0.35
Length of whole pipe/mm	241.5
Helix Pitch/mm	1.1
Helix Radius/mm	1.0
Helix pitch angle/ (°)	9.9
Peak magnetic field/T	0.905

3.2 Simulation Analysis of *K*-Means Clustering Algorithm

The original particles are simplified into different numbers of macroparticles, which are then used as the particle source for beam-wave interaction simulations of the TWT. Both the output power and the simulation time were recorded. The relationship between the number of macroparticles, the output power, and the simulation time is shown in Fig. 6. According to the Fig. 6, when the number of macroparticles ranged from 100 to 500, the output power of the interaction region showed little variation. A larger number of macroparticles resulted in longer simulation times. Therefore, the number of macroparticles should be kept as low as possible, when the output power is constant.

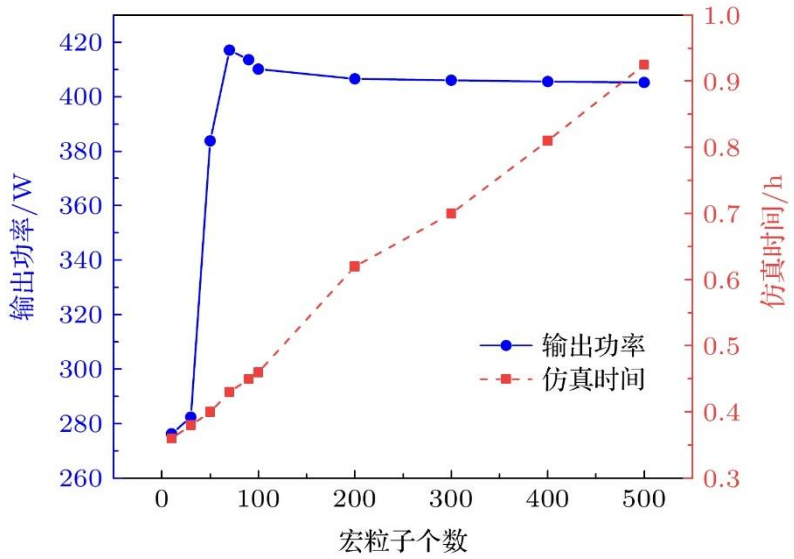

Figure 6. Relationship between the number of macro particles and the output power of the TWT as well as the simulation time.

The original particles are simplified using the *K*-mean clustering algorithm model, and the resulting macroparticles are shown in Fig. 7(a) and Fig. 7(b); The grid model is also used to simplify the original particles into the distribution of macroparticles. In the Fig. 7(c), the *x*-axis and *y*-axis are each divided into 12 equal segments, resulting in 144 equal grid regions. The particle parameters in each small equal grid are simplified into a new macroparticle through a unified calculation. The final simplified distribution of 112 macroparticles obtained via the grid model is shown in Fig. 7(d). To compare the output results with those of the grid model, the number of macroparticles generated by the *K* means clustering algorithm is also set to 112.

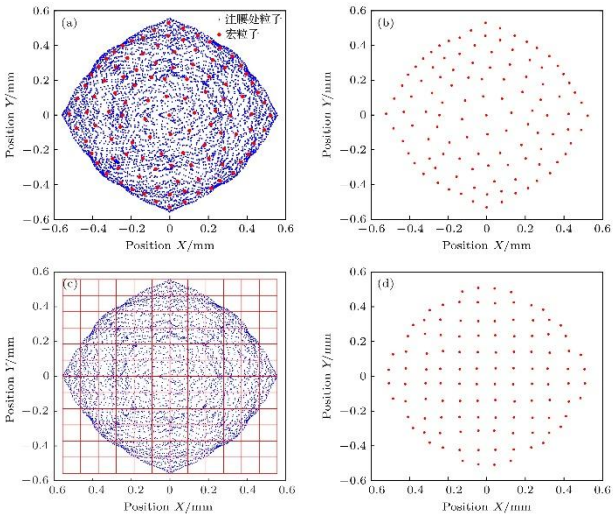

Figure 7. Particles at the waist of the electron gun are simplified into macroparticles by using the *K*-means clustering algorithm and the mesh model: (a) The cross-sectional particles are processed by using the *K*-means clustering algorithm; (b) the distribution of the macro particles after simplification by using the *K*-means clustering algorithm; (c) the cross-sectional particles are processed by using the mesh model; (d) the distribution of the macro particles after simplification by using the mesh model.

By varying the input signal power of the TWT, the original particles, the macroparticles simplified by the *K*-mean clustering algorithm, and those simplified by the grid model are each used as the particle sources for beam-wave interaction simulation. The output powers corresponding to different input powers are obtained. The results are shown in Fig. 8. From Fig. 6 and Fig. 8, it can be seen that when the power of the input signal is 6.8 mW, 4963 original particles are used, the simulation time is 5.53 h, and the output power is 404.73 W. When the particle source simplified by the *K*-mean clustering algorithm contains 112 macroparticles, the simulation time is 0.65 h, and the output power is 405.25 W, which is only 0.52 W higher than that of the original particles. Using the simplified grid model with 112 macroparticles as the particle source, the simulation time is the same as 0. 65 h, but the output power of the TWT is 416.88 W, which is 11.63 W higher than that obtained with the original particle source. It can also be seen from theFig. 6 and Fig. 8 that, compared with the unsimplified original particles, both the *K*-means clustering algorithm and the mesh model significantly reduce the computational load of the interaction region simulation. Compared with the grid model, the beam-wave interaction simulation results obtained from macroparticles generated by the *K*-means clustering algorithm are closer to those obtained from the original particles.

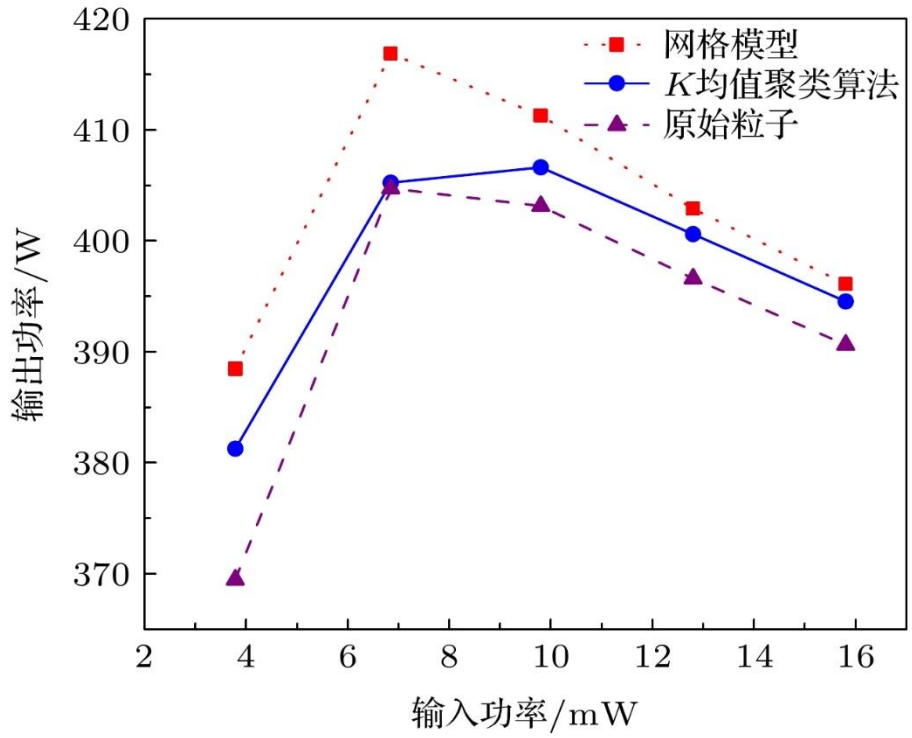

Figure 8. Output power under signals with different input powers.

3.3 Effect of electron beam laminarity on the TWT interaction region

Based on the simplification of *K*-means clustering algorithm, the laminar state of the electron beam at the beam waist can be easily and efficiently reflected in the beam-wave interaction of the TWT. In this paper, two parameters, the divergence angle of the cathode particles and the distance between the cathode and the anode, are adjusted as an application example to study the laminar flow of the electron beam. By varying these parameters, the laminar flow characteristics are altered, and the resulting effects on the output performance of the TWT are further analyzed.

3.3.1 Effect of electron gun cathode divergence angle on beam-wave interaction

The roughness of the cathode surface affects the initial electron emission angle. This cathode roughness is modeled by setting the distribution of the electron divergence angle[21]. Beam-wave interaction simulations are performed using particles obtained under different divergence angles at the electron gun cathode. The relationship between the divergence angle and the output power of the TWT is shown in the Fig. 9. When the cathode surface is so rough that the divergence angle of the particle source is between 0 ° and 0.4 °, the radial RMS emittance changes little, the electron beam laminarity changes little, and the output power of the TWT decreases slightly, remaining above 390 W. When the cathode surface is so rough

that the divergence angle is between 0.4 ° and 0.6 °, the radial RMS emittance increases significantly, the laminar flow is affected, and the output power of the TWT decreases markedly, falling below 390 W. When the cathode surface is so rough that the divergence angle increases from 0.6 ° to 1 °, the radial RMS emittance increases to the maximum, the electron beam has the poorest laminar flow, and the output power decreases sharply to 63 W. In general, a rougher cathode surface—i.e., a larger divergence angle—leads to a higher radial RMS emittance, indicating worse electron beam laminarity and consequently a reduction in the output power of the TWT.

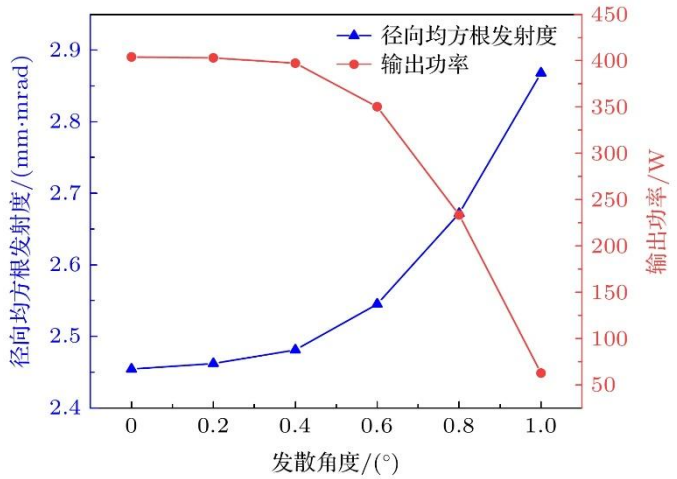

Figure 9. Relationship of the divergence angle of the particle source of the actual electron gun to the radial rms-emittance and the output power of the TWT.

3.3.2 Effect of distance between cathode and anode of electron gun on beam-wave interaction

Adjusting the distance between the cathode and the anode of the electron gun affects the electric field intensity and the space charge effect, thereby influencing the quality of the electron beam. This adjustment also impacts the emission current and consequently the perveance of the electron gun. To maintain a constant perveance, the emission current was kept at 0.35 A by adjusting the cathode emission area.

Simulations are conducted with the cathode–anode distance varying from 0.4 mm to 2.0 mm. The resulting transverse and longitudinal velocities of the particles are obtained, and the influence of the cathode–anode distance on these velocities is shown in Fig. 10. It can be seen that the average transverse velocity of particles in the electron beam fluctuates in the range of 4.2×10^5 — 4.65×10^5 m/s, indicating a relatively small variation range. Where $v_t = \sqrt{v_x^2 + v_y^2}$; the average longitudinal velocity of particles in the electron beam fluctuates in the

range of 5.670 $\times 10^7$ — 5.678 $\times 10^7$ m/s, also showing a narrow range of variation.

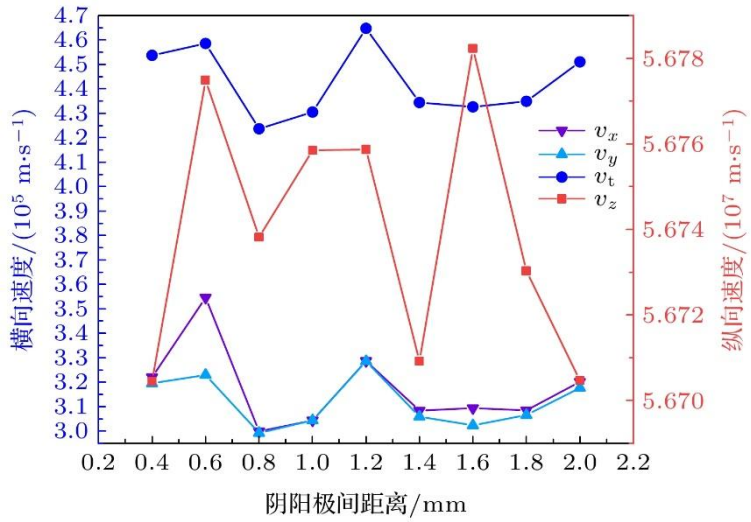

Figure 10. Influence of the distance between the anode and cathode on the transverse and longitudinal velocities of particles.

When only the average transverse velocity at the particle source is varied, the effect of the transverse velocity on the output signal gain of the TWT, obtained by the beam-wave interaction simulation, is shown in Fig. 11. When the average transverse velocity varies in the range of 4.2 $\times 10^5$ to 3.5 $\times 10^6$ m/s, the gain of TWT decreases with the increase of transverse velocity. When the distance between the cathode and the anode of the electron gun is adjusted and the average transverse velocity fluctuates in the range of 4.2 $\times 10^5$ to 4.65 $\times 10^5$ m/s, the change of the gain of the traveling wave tube is about 0.004 dB, and the change is small. It can be seen that the change of particle transverse velocity caused by adjusting the distance between the cathode and anode of the electron gun has a limited effect on the gain of the traveling wave tube. MATLAB is used to process the particle information, increase the average longitudinal velocity at the particle source, and simulate the beam-wave interaction. The influence of the particle longitudinal velocity on the output signal gain of the traveling wave tube is shown in the Fig. 12. When the average longitudinal velocity increased from 5.670 $\times 10^7$ m/s to 5.76 $\times 10^7$ m/s, the gain of the traveling wave tube increases first and then decreases. By adjusting the distance between the cathode and anode, the average longitudinal velocity of particles fluctuates in the range of 5.670 $\times 10^7$ — 5.678 $\times 10^7$ m/s. The gain of the traveling wave tube is more than 46 dB, with a variation of only 0.1 dB. Therefore, changes in longitudinal velocity due to adjustments in the cathode–anode distance also have a limited impact on TWT gain. Since both individual transverse and longitudinal velocity variations

have little effect on TWT gain when the cathode–anode distance is adjusted, further simulation studies are required from the perspective of electron beam laminarity.

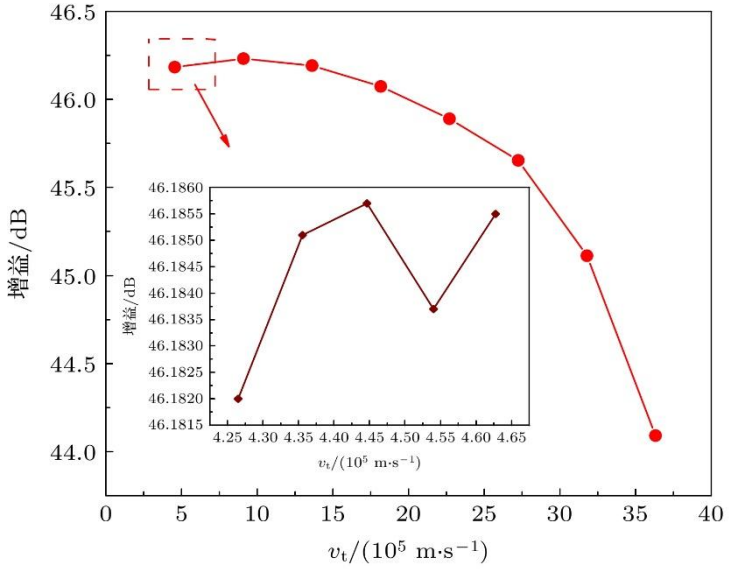

Figure 11. Influence of the transverse velocity of particles on the output signal gain of the TWT.

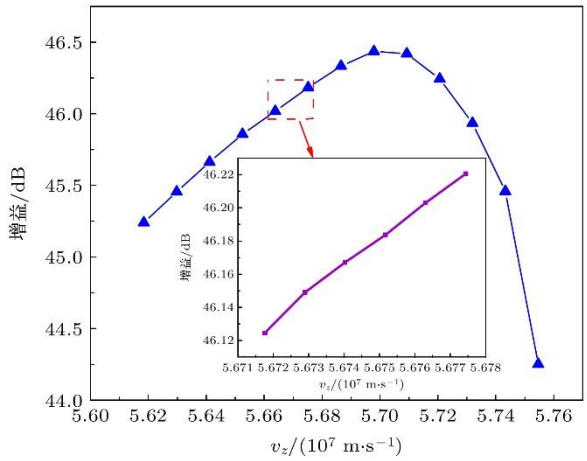

Figure 12. Influence of the longitudinal velocity of particles on the output signal gain of the TWT.

Electron guns with the distances between cathode and anode of 0. 4, 0.8, 1.2, 1.6, 2 mm were selected. The particles at the beam waist of each electron beam were used as the particle source for TWT beam-wave interaction simulations. When the input signal power was 9. 8 mW, the relationship between the cathode-anode distance, the radial RMS emittance of the electron beam, and the output power of the TWT was obtained as shown in Fig. 13.

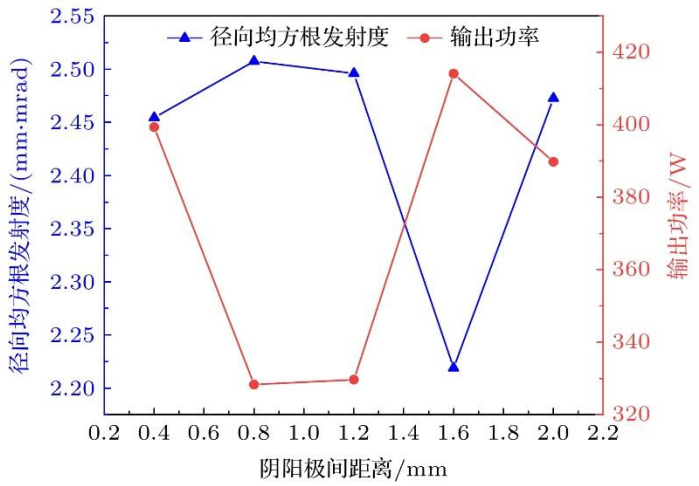

Figure 13. Influence of the distance variation between the anode and cathode on the radial rms-emittance of the electron beam and the output power of the TWT.

When the cathode-anode distance is 1.6 mm, the radial RMS emittance reached its minimum value of 2.22 mm·mrad, indicating the best laminar flow of the electron beam, and the output power reached its maximum of 414.10 W. When the distance was 0.8 mm, the radial RMS emittance peaked at 2.51 mm·mrad, corresponding to the worst laminar flow, and the output power dropped to its minimum of 328.34 W. It can be seen from the Fig. 13 trend that a larger radial RMS emittance corresponds to poorer electron beam laminarity and, consequently, lower TWT output power.

Two representative cases—corresponding to the worst and best electron beam laminarity (cathode–anode distances of 0.8 mm and 1.6 mm, respectively)—are selected as the particle source. Only the frequency of the input signal is varied, and the gain and bandwidth of the TWT are studied under different laminar flow conditions. When the distance between cathode and anode is 0. 8 mm and 1. 6 mm, the relationship between the input signal frequency and the output power of the TWT is shown in the Fig. 14. The electron beam with better laminar flow consistently produced higher output power across all input signal frequencies. It can be seen from the Fig. 14 that when the cathode–anode distance was optimized to 1.6 mm, the TWT output power exceeded 200 W over a bandwidth of 7 GHz (from 7 GHz to 14 GHz), and exceeded 300 W over a bandwidth of 5 GHz (from 9 GHz to 14 GHz). In contrast, with a cathode–anode distance of 0.8 mm, the output power exceeded 200 W over a bandwidth of 4 GHz (from 8 GHz to 12 GHz), and exceeded 300 W over a bandwidth of 3 GHz (from 9 GHz to 12 GHz). These simulation results demonstrate that radial RMS emittance is an effective parameter for characterizing the laminar nature of the electron beam. Better laminar flow leads to higher output signal gain, greater output power, and wider operating bandwidth, thereby continuously optimizing the overall output characteristics of the TWT. Using radial RMS emittance to evaluate electron beam laminarity provides valuable guidance for the

structural optimization design of the electron gun.

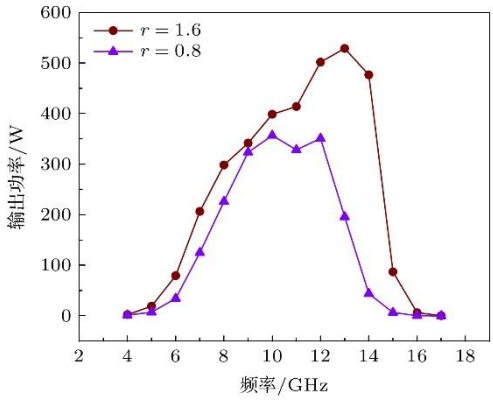

Figure 14. Relationship between the input signal frequency and the output power of the TWT when the distance between the anode and cathode is 0.8 mm and 1.6 mm respectively.

4. Conclusion

The particles at the beam waist of the electron gun are simplified into macro particles by using the *K*-means clustering algorithm, and the number of particles is reduced, so that the simulation time of the beam-wave interaction is reduced from 5. 53 h to 0. 65 h, and the method effectively reduces the simulation time of the beam-wave interaction. Compare with that grid model, the output obtained by the *K*-means cluster algorithm is closer to the output obtained by the original particle. By adjusting the parameters of the electron gun, the particle information at the beam waist of the electron beam with different laminar flow characteristics is obtained. The beam-wave interaction simulation results show that the radial RMS emittance can be used to characterize the laminarity of the cylindrical electron beam. By adjusting the distance between the cathode and anode of the electron gun, the laminar flow of the electron beam is improved, the radial RMS emittance is reduced, the output power of the space TWT is increased from 328. 34 W to 414. 10 W, and the operating frequency bandwidth for output power greater than 300 W is extended from 3 GHz to 5 GHz. Therefore, the change of electron beam laminar flow will affect the output power and operating bandwidth of the TWT, and the influence of electron beam laminar flow on the performance of the TWT can guide the optimization of the structural parameters of the electron gun. A larger divergence angle of the particle source leads to a higher radial RMS emittance, indicating poorer electron beam laminarity and resulting in a decrease in the gain of the TWT output signal. The *K*-means clustering algorithm is used to simplify the original particles, which reduces the simulation time and ensures the accuracy of the simulation results. Although the current application of

the clustering algorithm is primarily aimed at accelerating simulations, future work should focus on experimentally testing the optimized electron gun and TWT, as well as investigating the latest advancements in clustering algorithms. This will help improve the precision of using clustering algorithms to assist in the design and optimization of TWTs.

References

[1] Guo Z, Zhang R, Lai H, Lan F, Wang Z, Lu Z 2023 IEEE Trans. Electron Devices 70 2753

[2] Feng X X, Liao G X, Chen H X, Su Y S, Luo C C 2024 Proceedings of the 22nd Academic Conference on Vacuum Electronics Guangzhou, China, May 9, 2024 p2

[3] Pan R, Zhong C, Qian J 2024 IEEE Trans. Ind. Inf. 20 5914

[4] Hou J, Zhang A 2020 IEEE Trans. Ind. Inf. 16 2477

[5] Fang X, Xu Z, Ji H, Wang B, Huang Z 2023 IEEE Trans. Ind. Inf. 19 5476

[6] Jiang Z, Lin R, Yang F, Wu B 2018 IEEE Trans. Ind. Inf. 14 1856

[7] Jain A K 2010 Pattern Recognit. Lett. 31 651

[8] Wang J, Shen C, Zhang J, Fan H, Bai N, Sun X 2023 International Vacuum Electronics Conference Chengdu, China, April 25–28, 2023 p1

[9] Carlsten B E, Nichols K E, Shchegolkov D Y, Simakov E I 2016 IEEE Trans. Electron Devices 63 4493

[10] Ge X, Xu J, Yue L, Yin H, Zhao G, Wang W 2020 International Vacuum Electronics Conference Monterey, CA, USA, October 19–22, 2020 p237

[11] Shen C, Bai N, Zhang J, Sun X, Fan H 2019 International Vacuum Electronics Conference Busan, Korea (South), April 28–May 01, 2019 p1

[12] Louksha O, Trofimov P, Malkin A 2023 International Vacuum Electronics Conference Chengdu, China, April 25–28, 2023 p1

[13] Zhang J, Geng Z, Jin Q 2022 J. Phys. Conf. Ser. 2290 012030

[14] David J, Ives R L, Tran H T, Bui T, Read M E 2008 IEEE Trans. Plasma Sci. 36 156

[15] Liu W, Liu S 2011 Front. Electr. Electron. Eng. Chin. 6 556

[16] Shen C, Wang J, Zhang J, Feng J, Sun X 2022 IEEE Trans. Plasma Sci. 50 2830

[17] Lund S M, Kikuchi T, Davidson R C 2009 Phys. Rev. Spec. Top. Accel. Beams 12 114801

[18] Zhao G Q, Yue L N, Wang W X, Gong Y B, Wei Y Y, Huang M Z 2008 High Power Laser Part. Beams 20 1159

[19] Stockli M P, Welton R F, Keller R 2004 Rev. Sci. Instrum. 75 1646

[20] Whaley D R 2014 IEEE Trans. Electron Devices 61 1726

[21] Li D 2024 M. S. Thesis (Chengdu: University of Electronic Science and Technology of China